

Modes of Disintegration of Solid Foods in Simulated Gastric Environment

Fanbin Kong · R. Paul Singh

Received: 8 January 2009 / Accepted: 20 May 2009 / Published online: 23 June 2009
© The Author(s) 2009. This article is published with open access at Springerlink.com

Abstract A model stomach system was used to investigate disintegration of various foods in simulated gastric environment. Food disintegration modes and typical disintegration profiles are summarized in this paper. Mechanisms contributing to the disintegration kinetics of different foods were investigated as related to acidity, temperature, and enzymatic effect on the texture and changes in microstructure. Food disintegration was dominated by either fragmentation or erosion, depending on the physical forces acting on food and the cohesive force within the food matrix. The internal cohesive forces changed during digestion as a result of water penetration and acidic and enzymatic hydrolysis. When erosion was dominant, the disintegration data (weight retention vs. disintegration time) may be expressed with exponential, sigmoidal, and delayed-sigmoidal profiles. The different profiles are the result of competition among the rates of water absorption, texture softening, and erosion. A linear-exponential equation was used to describe the different disintegration curves with good fit. Acidity and temperature of gastric juice showed a synergistic effect on carrot softening, while pepsin was the key factor in disintegrating high-protein foods. A study of the change of carrot microstructure during digestion indicated that degradation of the pectin and cell wall was responsible for texture softening that contributed to the sigmoidal profile of carrot disintegration.

Keywords Stomach · Food digestion · Disintegration · Texture · Microstructure · Modeling

Introduction

Recent developments in food processing have focused on manufacturing foods for healthy benefits such as targeting release of nutrients in desired sites of the human gastrointestinal (GI) tract. For this purpose, it is critical to understand how foods break down during digestion in the GI tract. The stomach is a major compartment where the size of food particulates is reduced after oral mastication. From an engineering perspective, the stomach is a receptacle, a grinder, a mixer, and a pump that controls the digestion process.¹ The knowledge and any capability to predict how a food may disintegrate in the stomach are important for developing new food products with novel health benefits. However, there remains a notable lack of understanding about the kinetics of food disintegration and its relation to food texture and microstructure (that define the material properties) resulting from various food processing.

Studies in medicine, pharmacy, and nutrition have demonstrated that disintegration of food in the stomach is a complex process. Food is broken into small particulates and molecules due to both physical forces and chemical reactions.^{1,2} Physical forces include mechanical and hydrodynamic forces present in the stomach, resulting from the peristaltic movement of the stomach wall. Stomach contractions generate fluid flow of the gastric content that cause a shearing effect on the food surface.³ Kinetics of food digestion depend on the chemical and physical characteristics of food. Our previous study has shown that food disintegration rate is

F. Kong · R. P. Singh (✉)
Department of Biological and Agricultural Engineering,
University of California,
Davis, CA 95616, USA
e-mail: rpsingh@ucdavis.edu

F. Kong · R. P. Singh
Riddet Institute, Massey University,
Palmerston North, New Zealand

significantly affected by the initial texture and its change during digestion.⁴ However, more studies are needed to understand how the reactions occurring during digestion change food material properties and subsequently influence its disintegration.

In the stomach, gastric juice is secreted from glands lining the stomach containing gastric acid (HCl) and digestive enzymes. HCl assists acid denaturation of digested food and activates pepsin. In the fasted state, intragastric pH in healthy subjects is in the 1.3–2.5 range, while eating can increase pH up to 7.⁵ Gastric juice contains 0.8–1 mg/mL pepsin⁶ that degrades food proteins into peptides. The gastric juice penetrates the food matrix and assists in digestion, but how the acidity and enzyme of the gastric juice as well as temperature affect disintegration of food has not been fully understood.

We have developed a novel model of human stomach to study food disintegration kinetics.⁴ This model can provide measurable force that simulates the hydrodynamic and mechanical forces acting on foods *in vivo*. The objectives of this study were (1) to investigate disintegration characteristics and related mechanisms of different foods using the model system; (2) to study the role of temperature, acidity, and enzyme of gastric juice in food disintegration; and (3) to demonstrate how digestion changes food microstructure and subsequently influences its disintegration, using carrot as an example.

Materials and Methods

Materials and Sampling

Foods representing different categories were selected for this study (Table 1). Most of the foods were purchased in local grocery stores. Baked and fried dough products were prepared in the laboratory. Dough was prepared using wheat flour (Gold medal, General Mills, MN, USA) and water in a ratio of 100:55 (flour/water) and mixed using a dough mixer (Classic Series Tilt-Head Stand Mixer, KitchenAid, St. Joseph, MI, USA) for 10 min. After resting for 30 min, the dough was flattened into thin sheets of

1.5 cm thickness and baked in an oven (Hamilton Beach Brands, Inc., Washington, NC, USA) at 170°C for 30 min. Fried dough was prepared by cutting cylindrical samples (diam 10 mm×10 mm length) from the dough sheet and fried in an electric deep fryer (Presto FryDaddy, National Presto Industries, Inc. Eau Claire, WI, USA) at 180°C for 6 min. Broiled beef steak was prepared by heating 2.5-cm thick sirloin steak in an oven at 190°C for 8 min.

The food sample size for disintegration trials was determined according to observations and literature values reported on the particle sizes after oral mastication.^{7, 8} Beef jerky, peanut, almond, fried dough, bread crouton, and broiled beef steak were carefully cut into small samples with length 3–6 mm depending on the original shape and dimensions. Cylinder samples (6 mm diam×6 mm length) were obtained from carrot using a core cutter.

Simulated gastric juice and saliva were prepared as described in a previous paper.⁴ All chemicals were purchased from Sigma-Aldrich, Inc. (USA).

Model Stomach System and Disintegration Test

The model stomach system described in our previous paper⁴ was slightly modified. A stainless steel annular container was placed in the center of the glass chamber. The simulated gastric juice and plastic beads were filled in the annular container. This modification improved the uniformity of temperature in the simulated gastric juice and allowed easy addition and removal of beads and gastric juice (Figure 1). The sample holder arm was also modified to contain four sample hooks so as to accommodate four samples at the same time.

The operating procedures were described in our previous paper.⁴ The samples were first soaked in the simulated saliva for 30 s (37°C) to incorporate the effect of oral step on food disintegration. Then, the samples were hooked in each sample holder. Glue (Loctite super glue, Henkel Consumer Adhesives, Inc., Avon, OH, USA) was applied to fix samples when necessary. The samples were subjected to a continuous force in the model and the weight changes were measured periodically with a time interval between 1 and 30 min depending upon the disintegration rate. Weight retention ratio was calculated as:

$$y_t = \frac{W_t}{W_0} \quad (1)$$

where W_0 is initial weight (gram) and W_t (gram) is the sample weight after time t (minute). In this equation, it should be noted that W_t represents the weight of sample due to the

Table 1 Foods selected for disintegration study

Category	Foods
Meat products	Beef jerky, ham steak, broiled beef steak
Nuts	Raw peanuts, raw almonds
Fruits	Baby carrots
Baked products	Bread crouton, baked dough
Fried products	Fried dough products (w/o yeast)

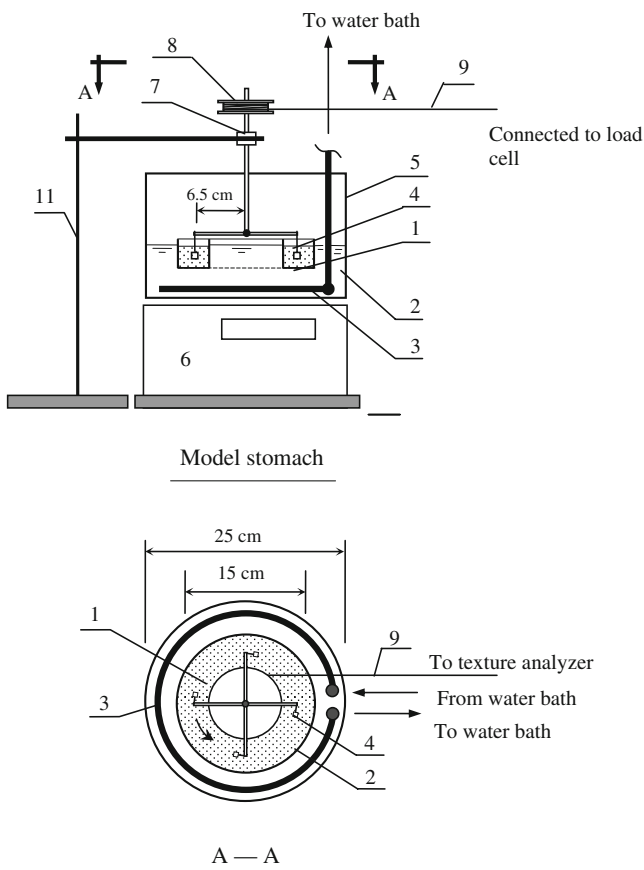


Fig. 1 Diagram of modified model stomach system and force measurement apparatus: 1 simulated gastric juice (37°C) and beads; 2 jacket filled with water; 3 copper coil; 4 food sample; 5 chamber; 6 turntable; 7 ball bearing; 8 wheel; 9 cotton wire; 10 pulley; 11 laboratory stand

simultaneous uptake of gastric juice and loss of its solid components due to disintegration and leaching.

Static Soaking Test

A static soaking test was employed to investigate water absorption and the change in texture of foods during digestion. Almond, carrot, and ham samples (10×10×4 mm) were soaked in simulated gastric juice at 37°C for 2 h. The weight changes were determined to calculate water absorption ratio. A penetration test was used to evaluate hardness of sample before and after soaking. A flat-ended needle probe (2 mm diameter) was fitted to the Texture Analyzer TA-XT2 (Texture Technologies Corp., Scarsdale, NY/Stable Micro Systems, Godalming, Surrey, UK) equipped with a load cell of 50 kg. The probe traveled to 2 mm depth into the planer surface of samples at a speed of 0.5 mm/s. The maximum force recorded during the test is referred to as the hardness of sample.

To investigate the water penetration in a carrot sample during digestion, methylene blue was added to the gastric

juice. During static soaking test of carrots, a visible region showing water penetration was clearly observed.

Microscopy Imaging

Light microscopy (LM) and transmission electron microscopy (TEM) were used to investigate changes in the microstructure of partially digested carrot. Carrot was soaked in simulated gastric juice for 20 min at 37°C. Samples were pre-fixed in Karnovsky's fixative (2.5% glutaraldehyde and 2.0% paraformaldehyde) in 0.08 mol/L phosphate buffer (pH 7.3). The tissues were secondarily fixed in 1% osmium tetroxide buffered in 0.1 M sodium phosphate buffer for 2 h. After thoroughly washing with cold double-distilled water, the samples were incubated in 0.1% tannic acid in water for 30 min on ice. Then, samples were rinsed three times with cold double-distilled water and incubated on ice in 2% aqueous uranyl acetate for 1 h. The rinsed tissue blocks were dehydrated using increasing concentrations of acetone: 10%, 30%, 50%, and 70% for 20 min each, followed by two changes of 95% acetone for 10 min each. The samples were embedded in a 100% Epon-araldite resin and polymerized overnight at 70°C.

The blocks were sectioned to obtain 400-nm-thick samples using a Diatome diamond knife. Dried sections were stained for 30–60 s using methylene blue and Azure B combination stain. The sections were rinsed, dried, coverslipped, and viewed on the LM. For the TEM, the block was trimmed to the area of interest (<1 mm), and 60-nm (silver) sections were cut and collected on a 150-mesh copper grid. They were dried and post-stained using the standard double staining protocol of 4% (w/v) uranyl acetate in 70% (w/v) aqueous methanol 20 min followed by lead citrate for 2 min. The sections were allowed to dry and viewed in a Philips 120 BioTwin Electron Microscope at 80 kV (Fei Company, Hillsboro, OR, USA) equipped with a Gatan/MegaScan, model 794/20 digital camera (Gatan Inc., Pleasanton, CA, USA).

Data Analysis

Weight retention data (y_i vs. t) were analyzed and fitted into an empirical model. Modeling of data was performed with nonlinear and multiple regression analysis functions of Excel software. Estimates for parameters were obtained by minimizing the mean square error (MSE):

$$\text{MSE} = \frac{\sum_{i=1}^n (y_i - \hat{y}_i)^2}{n} \quad (2)$$

where y_i is the observed value, \hat{y}_i is the fitted value, and n is the number of observation points of an experiment. MSE is a measure of the goodness of fit. In addition, the correlation

coefficient (r) is also used as a criterion for evaluating the performance of the models, and closeness to a value of 1 is an effective and practical measure of the validity of model prediction.

A significance test was conducted using analysis of variance (ANOVA) in the GLM procedure of the SAS System. Differences between group means were analyzed by Duncan's multiple range test. Statistical significance was set at a probability level of 0.05.

Results and Discussion

Fragmentation and Erosion

We observed two major mechanisms responsible for food disintegration in a simulated gastric environment, namely fragmentation and erosion. Fragmentation is the breakage of a food sample into several pieces of relatively large-size particulates. This phenomenon occurred when the applied stress is greater than a critical stress. The critical stress is related to the internal cohesive forces that hold the food matrix together. Surface erosion is defined as the wearing away of food surface by an impinging gastric fluid containing food solids that causes normal impact, friction, and shear forces acting on the food surface;⁴ it is the dominant mechanism when the applied stress is less than the critical stress. The erosion rate is therefore dependent upon the cohesive strength of the food matrix and the physical forces applied on the food.

Marciani et al.² measured stomach force exerted on agar gel beads (diameter 1.27 cm) and reported a maximum force of 0.65 N generated by the antral walls of a human stomach. The magnitude of the stomach forces is influenced by biological factors such as age, body mass index, hormonal factor, gender, blood glucose level, posture, stress and depression, and diseased states. The stomach can also detect and react to the food properties such as viscosity by increasing or decreasing the force of contraction and thus generate an appropriate disintegration rate.⁹ Therefore, the disintegration mode for the same food may vary significantly depending on an individual person. An advantage of our model stomach system is its ability to adjust the mechanical force applied on food samples by changing the concentration of beads added to the simulated gastric juice thus to simulate the disintegration of foods for a wide range of forces. To compare the disintegration mode of various foods, we tested different foods at the same force of about 0.25 N on a cylindrical sample (6 mm diam × 6 mm length) which is approximately in a similar range of the maximum force generated by the movement of the stomach wall. The applied force was controlled by operating the apparatus at the same rotational speed (30 rpm), and using

the same amount of gastric juice (176 mL) and beads (324 g), which made up 500 mL of simulated gastric content. Our preliminary observations showed that the disintegration mode varied greatly among different foods and was closely related to the initial food texture and its change during oral mastication and stomach digestion. Fragmentation dominated the disintegration of bakery products, such as a fried snack food, crouton, and baked dough. They became soft and easy to break apart after combination of saliva and gastric juice. Meat products, such as broiled beef steak, also demonstrated mainly fragmentation during digestion, as the connective tissue were denatured during roasting, and the muscle fibers were disconnected. Erosion was the major mechanism for the disintegration of carrot and nuts.

Higher force induced faster erosion rate, and an exponential relationship was observed between half time ($t_{1/2}$) and the applied mechanical force.⁴ Increase in the mechanical forces applied on food may also change the disintegration mode from erosion to fragmentation. On the other hand, after ingestion, the food texture may change as a result of water absorption, acid hydrolysis, and enzymatic reaction, leading to a reduction in cohesive forces that hold a food matrix together. Subsequently, the dominant disintegration mechanisms may shift from erosion to fragmentation. Figure 2 shows how a piece of crouton (7 mm length, weight 0.16 g) disintegrated in the model which contains only gastric juice when a force of 0.02 N was applied on the sample at the beginning of the trial. It shows that initially the crouton disintegrated by erosion (Figure 2a, b). Water absorption led to significant swelling and increase in its volume and softening of its texture. After about 30 min, the sample broke at the place close to the hook (Figure 2c), indicating that the cohesive force decreased due to water absorption and it was lower than the applied force. It is recognized that erosion and fragmentation may also occur simultaneously to disintegrate foods. Future studies will require understanding the critical stress of various foods and the relationship with food material properties, as well as their change during stomach digestion. In the following sections of this paper, we will focus on erosion, although the term "disintegration" will be used throughout the paper to represent the change of sample weight in the model stomach system.

Food Disintegration Profiles and Modeling

In our previous paper,⁴ we reported that the disintegration profile of carrot and ham showed either an exponential or sigmoidal decay. Specifically, the retention of the mass of raw carrot during disintegration trial followed a sigmoidal decrease with an early stage of slow disintegration, a second stage of increased disintegration, and a third stage of diminishing disintegration rate. An exponential decay

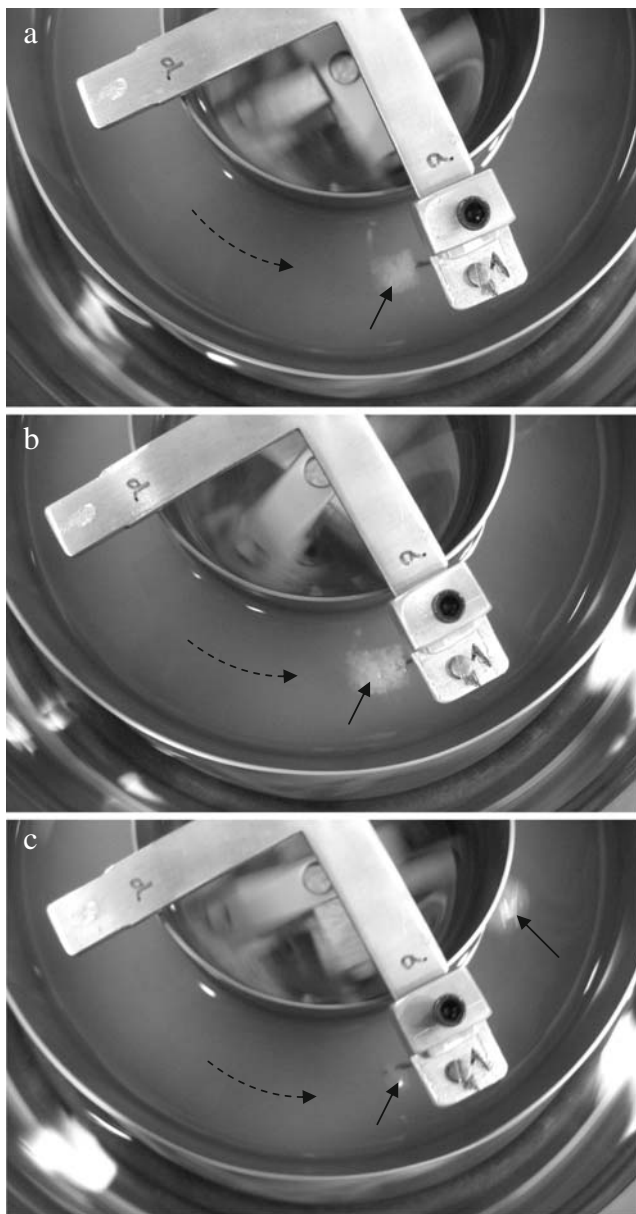


Fig. 2 Disintegration of bread crouton in the model stomach system: **a** erosion was the dominant mechanism in the beginning; **b** swelling of the sample; **c** rupture of the bread crouton after half hour of running. *Dashed arrow*: fluid rotational direction; *continuous arrow*: sample

with a rapid initial disintegration was observed in ham. The difference in the disintegration curves was hypothesized due to the competition between surface erosion and texture softening.⁴

Disintegration studies of additional types of foods have revealed another type of food disintegration profile, which is different from the two profiles previously suggested. In certain cases, we observed that the sample weight initially increased, leading to a weight retention ratio y_t higher than 1, and then it gradually decreased. This profile is named as a *delayed-sigmoidal* curve, when after an initial increase, the weight

retention ratio decreased following a sigmoidal profile. Delayed-sigmoidal type of disintegration mainly occurred for low-moisture food products, such as peanut, almond, and beef jerky. During digestion, a significant amount of water was absorbed that exceeded the weight loss due to erosion, leading to an increase in the sample weight and volume. In vivo studies have shown that dietary oat can absorb water and swell in stomach causing stomach distension and affecting satiety.¹⁰ However, a quantitative characterization of this phenomenon is lacking in the literature. Gamma scintigraphy, which is commonly used clinically to evaluate gastric emptying by counting the radioactivity of marked foods, cannot measure the meal volume in the stomach. Recent improvements in MRI may allow in vivo measurement of gastric and meal volumes.^{9,11}

Siegel's modified power exponential equation, which was proposed to describe in vivo stomach emptying data,¹² was used to fit the data obtained for carrot and ham in our previous study:⁴

$$y_t = 1 - (1 - e^{-kt})^\beta \quad (3)$$

In describing stomach emptying profile, y_t is the fractional food retention at time t (minute), k is a parameter related to the gastric emptying rate per minute, and β is a shape factor. This model, however, cannot describe the delayed-sigmoidal profile. Therefore, we propose the use of a linear-exponential equation for describing the three different profiles observed in food disintegration:

$$y_t = (1 + k\beta t)e^{-\beta t} \quad (4)$$

In this expression, k and β are constants. k is dimensionless and it represents the lag phase. A larger k is associated with a delayed-sigmoidal disintegration and a smaller k represents an exponential decay. β (1/min) is a parameter that measures the concavity of the weight retention vs. time relationship ($\beta > 0$). The pre-exponential term, $(1+k\beta t)$, generally predominates for a short time at the beginning of disintegration trial. As the trial continues, the exponential factor $e^{-\beta t}$ induces concavity in the weight retention vs. time profile. This model has advantages over the modified exponential model (Eq. 3) in that it captures initial increase in y_t due to water absorption. A similar model was proposed by Goetze et al.¹¹ to describe changes in the volume of stomach due to accommodation of food and secretion of gastric fluid. The k and β values can be derived using regression analysis. When k and β are known, the half time, $t_{1/2}$, can be calculated by regression analysis and using $y_t=0.5$.

Figure 3 shows typical delayed-sigmoidal disintegration profiles for beef jerky and raw almond as well as the model curves fitted with Eq. 4. Disintegration type, model parameters, and half times for some representative foods

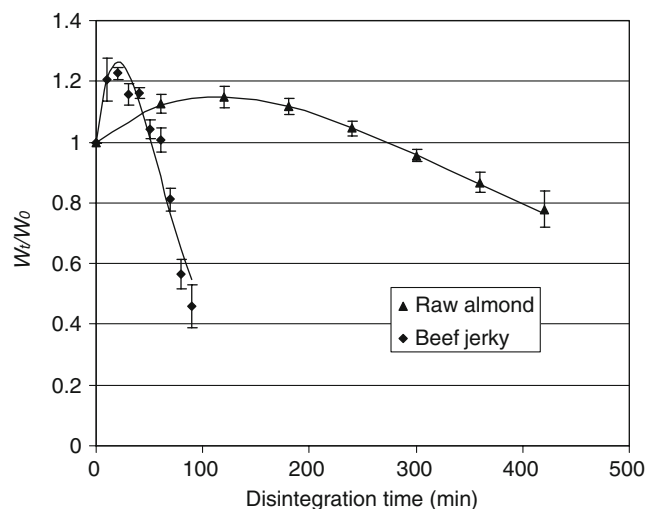


Fig. 3 Typical delayed-sigmoidal disintegration curves ($n=4$). Trial condition, 500 mL of simulated gastric content (gastric juice 176 mL, beads 324 g); turntable rotation speed, 30 rpm

tested in the stomach system are presented in Table 2. The MSE and r values indicate a good fit of the model equation with the disintegration data. It can be seen that the half time varies significantly with different foods, from a few minutes up to 12 h, depending upon the texture and microstructure of tested foods. It should be noted that although Eq. 4 provides a good fit of the data of three disintegration profiles, it does not necessarily represent any specific mechanism. It is also important to acknowledge that in addition to surface erosion, leaching of solids may occur simultaneously that contributes to the change of sample weight. Thus the disintegration profiles summarized here and the model equation 4 describe the overall effect of weight change caused by absorption of gastric juice, surface erosion and release of the solids.

Reactions Occurring During Digestion That Affect Disintegration

To further elucidate the mechanisms that affect food disintegration rate, three foods were compared, namely almond, carrot, and ham, representing different types of

disintegration: delayed sigmoidal, sigmoidal, and exponential, respectively (Table 2). A static soaking test was conducted for the three foods to compare water absorption, volume change, and texture change. Almond absorbed the highest amount of water, from originally 3.3% to 30.7% after soaking (wet basis). This is in agreement with the different k values in Table 2 indicating that a greater water absorption occurred for almond ($k>1$) than carrot and ham ($k<1$). Furthermore, measurement of texture indicated that a significant reduction in the hardness occurred for almond and carrot but not for ham (Figure 4).

We postulate that water absorption, textual softening, and surface erosion are the major factors affecting the disintegration rate and thus influencing the type of the disintegration profile. Food is first chewed in the mouth, then swallowed and transited into stomach. In the stomach, gastric juice penetrates into a food particulate that softens its texture. The rate of water absorption depends on the physical properties of foods such as food porosity, composition, and material properties. A high rate of water absorption contributes to a delayed-sigmoidal disintegration profile. When gastric fluid carrying acid and enzyme is absorbed into the food, acid hydrolysis and enzyme degradation occur that further soften food texture and weaken internal bonds. Depending on the initial temperature of the food, heat transfer takes place to equilibrate the food temperature to 37°C, which is the optimum temperature for enzymatic activity for pepsin. All of these phenomena—water absorption, heat transfer, and acid and enzymatic reactions contribute to degradation of food texture (tenderization) and weaken the strength of the food matrix that improves the disintegration rate increases leaching of solids. The tenderization (or softening) starts from the food surface and gradually moves inside. When a physical stress is applied (including both mechanical and hydrodynamic forces), surface erosion occurs. The erosion rate depends on the physical force and the internal cohesive strength of the food matrix. The erosion is slow for rigid and tough foods but fast for foods with softer texture. The shape of the disintegration profile is largely a result of a competition between the penetration rates of tenderization

Table 2 Disintegration profiles and parameters of Eq. 4 for representative foods

	Disintegration profile	k	β (1/min)	MSE $\times 10^3$	r	$t_{1/2}$ (min)
Ham (\emptyset 6 \times L6 mm cylinder)	Exponential	0.484	0.260	2.181	1.00	4.3
Fried dough (6 \times 6 \times 6 mm)	Exponential	0	0.121	0.548	0.998	5.8
Carrot (\emptyset 6 \times L6 mm cylinder)	Sigmoidal	0.994	0.105	2.141	1.00	16.0
Beef jerky (6 \times 6 \times 4 mm)	Delayed-sigmoidal	2.16	0.027	3.89	0.97	94.9
Almond (6 \times 6 \times 4 mm)	Delayed-sigmoidal	1.785	0.004	1.051	1.00	598.6
Peanut (6 \times 6 \times 4 mm)	Delayed-sigmoidal	1.977	0.003	1.304	0.984	714.8

Trial condition, 500 mL of simulated gastric content (gastric juice 176 mL, beads 324 g); turntable rotation speed, 30 rpm

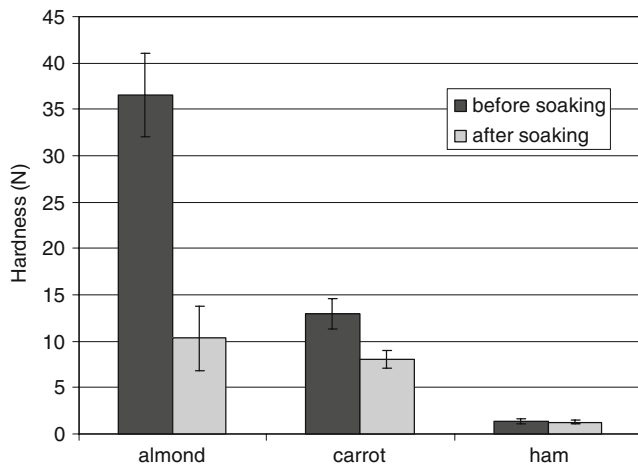


Fig. 4 Comparison of hardness changes in almond, carrot, and ham during static soaking test ($n=8$)

front and the erosion front resulting in the shrinking food surface. As can be seen in Table 2, foods with tough or rigid texture such as carrot and nuts tended to disintegrate with a sigmoidal or delayed-sigmoidal type profile because of their slow erosion rate. In case of almond, the significant water absorption and texture softening led to a delayed-sigmoidal profile of disintegration. For raw carrot, significant softening in the texture resulted in a sigmoidal curve, due to a faster moving tenderization front from surface to the center of the sample than the erosion front.⁴ Foods with softer texture, such as ham, tended to have an exponential profile due to their fast advancing erosion front that dominated during disintegration (Table 2). Fried dough was initially rigid, but became soft when it absorbed water during digestion, thus showing an exponential decay in the weight retention. On the other hand, ham showed no significant water absorption and textural change, resulting in an exponential decay of weight retention, mainly affected by a decrease of the surface area of the sample.⁴

For a given food, the disintegration profile may change among different categories when the applied force is changed. Larger force will cause faster erosion rate that contributes to an exponential profile. As can be seen in Figure 5, fried dough had a delayed sigmoidal curve at a lower force (0.07 N). However, when the force increased to 0.25 N, it shows an exponential decay in weight retention, indicating that at this force the erosion front proceeded faster than the rate of water penetration and texture softening. Similarly, 2-min cooked carrots showed a sigmoidal disintegration at lower force and an exponential decay of weight retention at higher force.⁴

Role of Acidity, Temperature, and Enzyme (Pepsin) on Food Disintegration: Synergistic Effect

As noted before, temperature change, acid hydrolysis, and enzymatic reaction play an important role in food disinte-

gration mainly through modifying food texture. Food ingestion may significantly change the composition of stomach content in terms of pH, temperature, and enzyme concentration. Upon ingestion of food, stomach secretes gastric juice, but it may take considerable time to recover to its original state, i.e., 1.5–2.5 of the pH, 37°C and pepsin concentration of ~1 g/L gastric juice.^{13,14} It was reported from *in vivo* studies that the pH of the gastric contents after ingestion of meal may rise to 5–7, and may take 1 h to fall to <3.0 and 2 h to return to <2.0.⁵ On the other hand, food enters the stomach in the form of bolus, and the breakdown of the bolus is by process of elution,⁹ in which meal dilution starts from the outer region and slowly moves towards the core of the bolus. Therefore, it may take a relatively long time (half hour or longer) for the solid particulates in the center of the bolus to get in contact with gastric juice. These *in vivo* studies indicate that ingested food particulates may not be immediately exposed to optimum gastric environment. The role of pH, temperature, and enzyme concentration on digestion needs to be fully understood.

We tested the role of pH, temperature, and pepsin on the disintegration of carrot and beef jerky. Disintegration of carrot samples was tested in the model stomach system containing fluid with different compositions of simulated gastric juice: (1) deionized (DI) water (pH=5.3), 21°C; (2) DI water, 37°C; (3) acidic water (pH1.8), 21°C; and (4) acidic water (pH1.8), 37°C. Half times of carrot disintegration in different fluids are shown in Figure 6a. Increase in the temperature and acidity significantly improved disintegration rate of carrot. An increase in temperature from 21 to 37°C led to a decrease in half time from 3.3 to 2.3 h, corresponding to a 30% increase in half time; while a change in pH from 5.3 to 1.8 resulted in a 55% decrease in

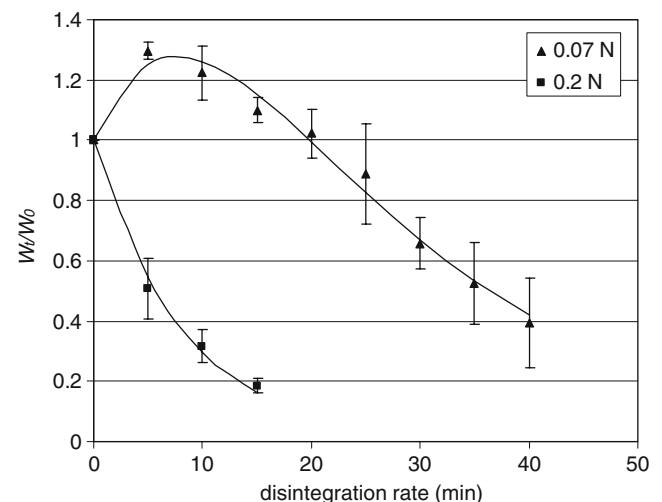


Fig. 5 Changes in the disintegration profile of fried dough under different forces applied in the model stomach system ($n=4$)

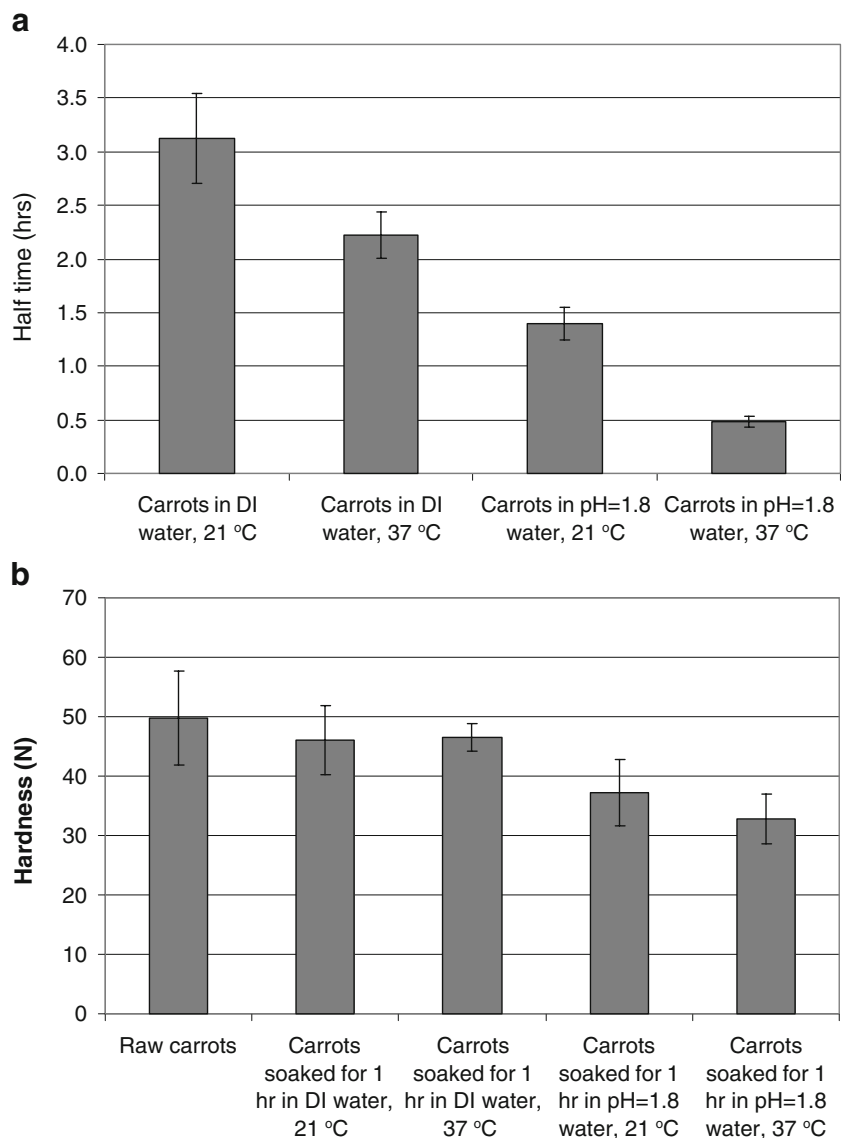
the half time (from 3.3 to 1.5 h). When both temperature and pH were adjusted, the half time decreased to 0.47 h, corresponding to 86% reduction. These results indicate a significant synergistic effect of pH and temperature for carrot disintegration. Figure 6b shows the hardness of carrot samples after soaking in different fluids. Generally, the half time (Figure 6a) and the hardness of soaked carrot (Figure 6b) have a good correlation: when carrots were soaked in water at 37°C and pH1.8 for 1 h, the hardness decreased the most, which resulted in the most rapid disintegration.

Figure 7 shows the half time of carrot disintegration in simulated gastric juice at four temperatures: 21, 29, 37, and 45°C. These temperatures were selected to cover the situations that may occur in the gastric environment for varying durations of time. The force applied was 0.13 N. The

half time decreased rapidly when the temperature increased from 21 to 45°C. A power relationship existed between half time and temperature. When temperature was higher than 37°C, the change in the rate of disintegration was minor.

Experiments comparing the disintegration of carrot in a simulated stomach environment with/without pepsin indicated that pepsin had no significant influence. However, the addition of 1% pepsin improved the disintegration rate of beef jerky by 21%, and the half time decreased from 1.9 to 1.5 h. This result was expected because pepsin functions to break up proteins into smaller peptides, while carrot contains only a small amount of protein (<1%) compared to beef jerky (~50%). It is also known that the optimum proteolysis of protein substrates by pepsin is achieved at pH of about 2.¹⁵

Fig. 6 Changes in the disintegration rates (a) and hardness (b) of carrots in different liquid media (n=8)



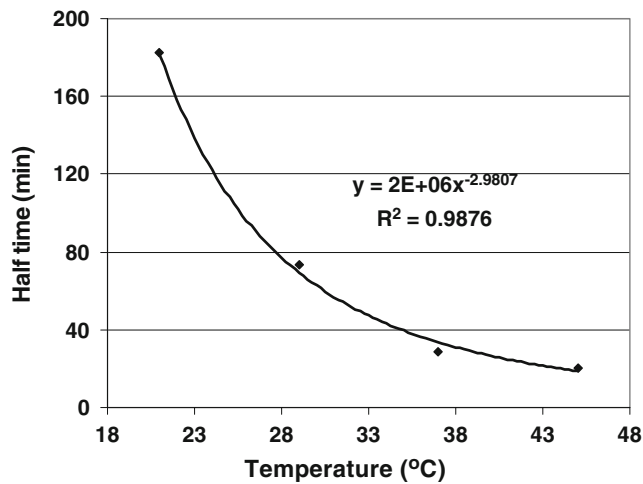


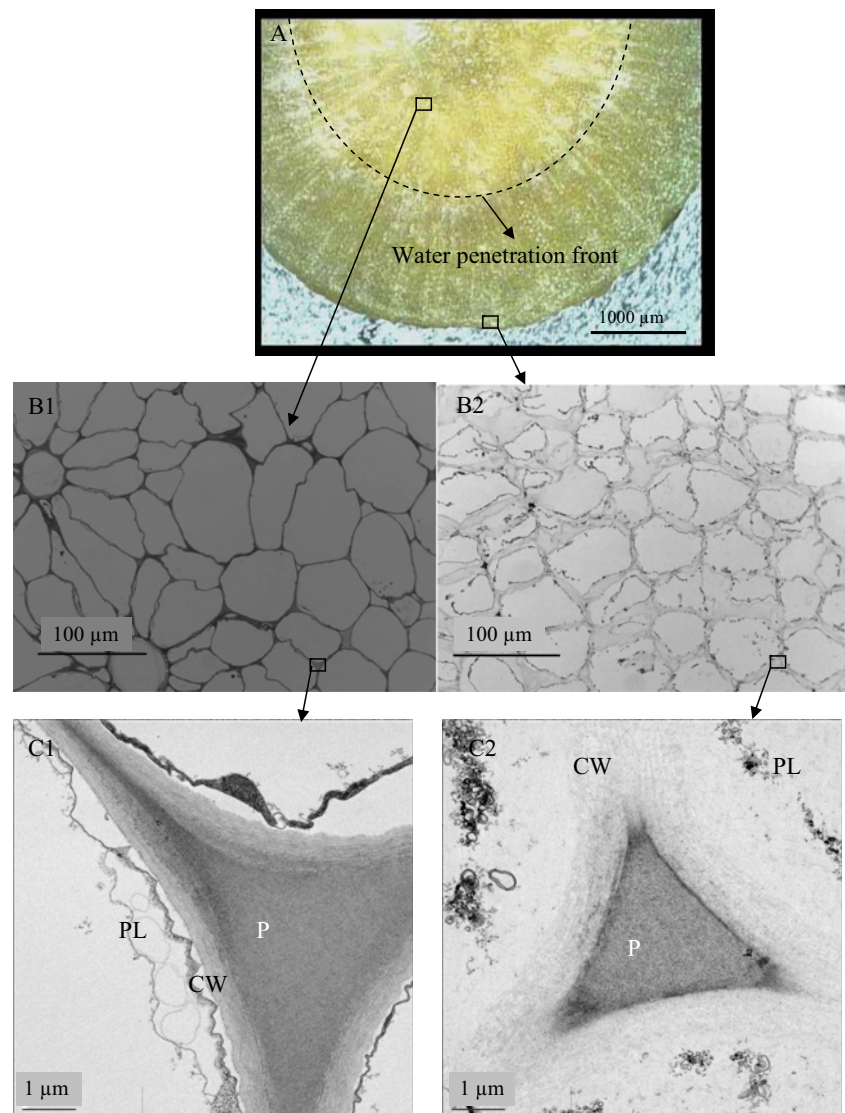
Fig. 7 Disintegration rates of carrot (expressed as half time) at different temperatures

Microstructure Changes in Carrots During Digestion

Food microstructure is expected to play an important role in the disintegration kinetics as well as the release and bioavailability of nutrients. For this study, we selected carrots to investigate how the microstructure changes in simulated gastric environment and its influence on disintegration. The microstructure of partially digested raw carrot after soaking in gastric juice for 20 min is shown in Figure 8. Methylene blue was added to gastric juice to determine the water penetration front by observing blue color in the water penetrated region where digestion occurred. A water penetration front can be seen, separating the cross-section of the carrot sample into an undigested central region (lighter) and a digested region closer to the surface (darker; Figure 8A). The different microstructures between these two areas are compared in Figure 8B1, B2, C1, and C2.

Fig. 8 Changes in the microstructure of digested carrots.

A Image showing cross-section of partially digested cylindrical carrot sample (diam 3 mm) and the front of water penetration indicated by dashed line (colored by methylene blue); *B1, B2* Light microscopy images showing the undigested central region and the severely digested edge region; *C1, C2* TEM images showing intact cell wall in the central region (*C1*) and damaged cell wall and dissolved pectin in the edge region (*C2*). *CW* cell wall, *PL* plasmalemma, *P* pectin



In the central region of the carrot sample, intact tissue can be seen composed of well-joined cells along their cell walls (Figure 8B1, C1). Cell wall comprises mainly of polysaccharides consisting of pectin, hemicellulose, and cellulose. Pectin polysaccharides are the major components in the middle lamella between plant cells and function as the intercellular cement that holds the cells together. The carrot texture is largely determined by the cell wall and pectin polysaccharides.¹⁶ In the region closer to the surface, a substantial degradation and solubilization of cell wall and pectin can be seen due to digestion (Figure 8B2, C2). Cell separation, cell wall damage, and plasmalemma breakage are visible in the digested region, as a result of acidic and enzymatic hydrolysis. Pectin loses some of its branching and chain length, resulting in reduced intercellular adhesion.¹⁷ Consequently, cell wall degrades and the cells separate that contribute to increased softening. These results indicate that the loss of texture in digested carrots, as shown in Figure 6b, was mainly caused by substantial dissolution, depolymerization, and destruction of cell wall polymers, particularly the pectic substances. Turgor loss caused by disruption of cell membranes may also have similar effect.¹⁸

When carrot, with its rigid texture, was tested in the stomach model, the erosion front (from the surface to the center) was moving at a slower rate than the penetration of gastric juice and tenderization. Thus, the texture of carrot surface gradually softened as disintegration continued, causing an increasing rate of disintegration. This disintegration rate, in combination with a reduction in the sample surface, resulted in a sigmoidal profile in carrot samples. These results support the findings of other researchers that in plant food tissues, the physicochemical structure and properties of the cell walls are critical factors that influence food breakdown in the GI tract, thus influencing the bioaccessibility of embedded nutrients.¹⁹

Conclusions

The dominant mode(s) of disintegration of solid foods in simulated gastric environment are fragmentation and/or erosion. These modes depend on the internal cohesive force of the food matrix which is closely related to the food texture and microstructure. The modes of disintegration also depend upon physical forces acting on the food due to peristaltic movement of stomach walls. For erosion-dominant disintegration, the weight retention ratio vs. disintegration time curve can be expressed with exponential, sigmoidal, and delayed-sigmoidal profiles. These profiles are influenced by the rates of erosion, water absorption, and degradation of texture. The three profiles were well described by a linear-exponential equation with two parameters. Water penetration along with acid hydro-

lysis and enzymatic action degrade the structural integrity of a food matrix, thus improving the disintegration rate. Acidity and temperature show a synergistic effect in softening food texture.

Acknowledgment The authors thank Mir Shafii and Ronald Budiman for their technical assistance. Microscopy imaging was conducted at Electron Microscopy Laboratory in the Department of Pathology and Laboratory Medicine, University of California, Davis. This research was supported in part by USDA-NRI, contract 2009-35503-05195.

Open Access This article is distributed under the terms of the Creative Commons Attribution Noncommercial License which permits any noncommercial use, distribution, and reproduction in any medium, provided the original author(s) and source are credited.

References

- J.L. Urbain, J.A. Siegel, N.D. Charkes, A.H. Maurer, L.S. Malmud, R.S. Fisher, The two-component stomach: effects of meal particle size on fundal and antral emptying. *Eur J Nucl Med* **15**, 254–259 (1989). doi:10.1007/BF00257543
- L. Marciani, P.A. Gowland, A. Fillery-Travis, P. Manoj, J. Wright, A. Smith, P. Young, R.J. Moore, R.C. Spiller, Assessment of antral grinding of a model solid meal with echo-planar imaging. *Am J Physiol* **280**, G844–G849 (2001)
- A. Pal, B. Abrahamsson, W. Schwizer, G.S. Hebbard, J.G. Brasseur, Application of a virtual stomach to evaluate gastric mixing and breakdown of solid food. *Gastroenterol* **124**, A673–A674 (2003). doi:10.1016/S0016-5085(03)83412-1
- F. Kong, R.P. Singh, A model stomach system to investigate disintegration kinetics of solid foods during gastric digestion. *J Food Sci* **73**(5), E202–E210 (2008). doi:10.1111/j.1750-3841.2008.00745.x
- W.N. Charman, C.J. Porter, S. Mithani, J.B. Dressman, Physicochemical and physiological mechanisms for the effects of food on drug absorption: the role of lipids and pH. *J Pharm Sci* **86**(3), 269–282 (2000). doi:10.1021/jps960085v
- M. Vertzoni, J. Dressman, J. Butler, J. Hempenstall, C. Reppas, Simulation of fasting gastric conditions and its importance for the *in vivo* dissolution of lipophilic compounds. *Eur J Pharm Biopharm* **60**(3), 413–417 (2005). doi:10.1016/j.ejpb.2005.03.002
- M.L. Jalabert-Malbos, A. Mishellany-Dutour, A. Woda, M.A. Peyron, Particle size distribution in the food bolus after mastication of natural foods. *Food Qual Prefer* **18**, 803–812 (2007). doi:10.1016/j.foodqual.2007.01.010
- M.A. Peyron, A. Mishellany, A. Woda, Particle size distribution of food boluses after mastication of six natural foods. *J Dent Res* **83**(7), 578–582 (2004). doi:10.1177/154405910408300713
- L. Marciani, P.A. Gowland, R.C. Spiller, P. Manoj, R.J. Moore, P. Young, A.J. Fillery-Travis, Effect of meal viscosity and nutrients on satiety, intragastric dilution, and emptying assessed by MRI. *Am J Physiol Gastrointest Liver Physiol* **280**, G1227–G1233 (2001)
- Y. Malkki, E. Virtanen, Gastrointestinal effects of oat bran and oat gum. A review. *Lebensm-Wiss Technol* **34**, 337–347 (2001). doi:10.1006/fstl.2001.0795
- O. Goetze, D. Menne, M. Kwiatek et al., Modeling of gastric volume data to assess gastric accommodation and emptying following ingestion of liquid meals. *Neurogastroenterol Motil* **17** (Suppl 2), 29 (2005). doi:10.1111/j.1365-2982.2004.00581.x

12. J.A. Siegel, J.L. Urbain, L.P. Adler, N.D. Charkes, A.H. Maurer, B. Krevsky, L.C. Knight, R.S. Fisher, L.S. Malmud, Biphasic nature of gastric emptying. *Gut* **29**(1), 85–89 (1988). doi:[10.1136/gut.29.1.85](https://doi.org/10.1136/gut.29.1.85)
13. J.B. Dressman, Comparison of canine and human gastrointestinal physiology. *Pharm Res* **3**(3), 123–131 (1986). doi:[10.1023/A:1016353705970](https://doi.org/10.1023/A:1016353705970)
14. F. Kong, R.P. Singh, Disintegration of solid foods in human stomach. *J Food Sci* **73**(5), R67–R80 (2008). Review. doi:[10.1111/j.1750-3841.2008.00766.x](https://doi.org/10.1111/j.1750-3841.2008.00766.x)
15. F.H. Kratzer, J.W.G. Porter, The effect of pH on the digestion of proteins in vitro by pepsin. *Br J Nutr* **16**, 579–584 (1962). doi:[10.1079/BJN19620056](https://doi.org/10.1079/BJN19620056)
16. J.V. Buren, The chemistry of texture in fruits and vegetables. *J Texture Stud* **10**, 1–23 (1979). doi:[10.1111/j.1745-4603.1979.tb01305.x](https://doi.org/10.1111/j.1745-4603.1979.tb01305.x)
17. R. Ilker, A.S. Szczesniak, Structural and chemical bases for texture of plant foodstuffs. *J Texture Stud* **21**, 1–36 (1990). doi:[10.1111/j.1745-4603.1990.tb00462.x](https://doi.org/10.1111/j.1745-4603.1990.tb00462.x)
18. L.C. Greve, K.A. Shackel, H. Ahmadi, R.N. McArdle, J.R. Gohlke, J.M. Labavitch, Impact of heating on carrot firmness: contribution of cellular turgor. *J Agric Food Chem* **42**(12), 2896–2899 (1994). doi:[10.1021/jf00048a047](https://doi.org/10.1021/jf00048a047)
19. P.R. Ellis, C.W. Kendall, Y. Ren, C. Parker, J.F. Pacy, K.W. Waldron, D.J. Jenkins, Role of cell walls in the bioaccessibility of lipids in almond seeds. *Am J Clin Nutr* **80**, 604–613 (2004)